



Universiteit
Leiden
The Netherlands

Spin-triplet supercurrents of odd and even parity in nanostructured devices

Lahabi, K.

Citation

Lahabi, K. (2018, December 4). *Spin-triplet supercurrents of odd and even parity in nanostructured devices*. *Casimir PhD Series*. Retrieved from <https://hdl.handle.net/1887/68031>

Version: Not Applicable (or Unknown)

License: [Licence agreement concerning inclusion of doctoral thesis in the Institutional Repository of the University of Leiden](#)

Downloaded from: <https://hdl.handle.net/1887/68031>

Note: To cite this publication please use the final published version (if applicable).

Cover Page



Universiteit Leiden



The handle <http://hdl.handle.net/1887/68031> holds various files of this Leiden University dissertation.

Author: Lahabi, K.

Title: Spin-triplet supercurrents of odd and even parity in nanostructured devices

Issue Date: 2018-12-04

6

LITTLE-PARKS OSCILLATIONS WITH HALF-QUANTUM FLUXOID FEATURES IN Sr_2RuO_4

Yasui, Yuuki and Lahabi, Kaveh and Anwar, Muhammad Shahbaz and Nakamura, Yuji and Yonezawa, Shingo and Terashima, Takahito and Aarts, Jan and Maeno, Yoshiteru

In a micro ring of a superconductor with a spin-triplet equal-spin pairing state, a fluxoid, a combined object of magnetic flux and circulating supercurrent, can penetrate as half-integer multiples of the flux quantum. A candidate material to investigate such half-quantum fluxoids is Sr_2RuO_4 . We fabricated Sr_2RuO_4 micro rings using single crystals and measured their resistance behavior under magnetic fields controlled with a three-axes vector magnet. Proper Little-Parks oscillations in the magnetovoltage as a function of an axially applied field, associated with fluxoid quantization are clearly observed, for the first time using bulk single crystalline superconductors. We then performed magnetovoltage measurements with additional in-plane magnetic fields. By carefully analyzing both the voltages V_+ (V_-) measured at positive (negative) current, we find that, above an in-plane threshold field of about 10 mT, the magnetovoltage maxima convert to minima. We interpret this behavior as the peak splitting expected for the half-quantum fluxoid states

This chapter has been published in *Physical Review B* **96**, 180507(R) (2017)

Author contributions: The crystals were grown in the group of Y. Maeno at Kyoto University. Y. Yasui and Y. Nakamura prepared the crystals. K. Lahabi and Y. Nakamura micro-structured the crystals under the supervision of T. Terashima. Y. Yasui, Y. Nakamura and K. Lahabi conducted the measurements. S. Yonezawa supervised and supported the measurements. Y. Yasui and K. Lahabi analysed the results. M. S. Anwar took part in the discussion. Y. Maeno and J. Aarts directed the project. All authors discussed the results and contributed to the final manuscript.

6.1. INTRODUCTION

Recently, it has been recognized that Majorana particles, which have unusual equivalence to their own antiparticles and have been long sought in elementary particle physics, can be realized as quasiparticle excitation in condensed-matter systems such as topological superconductors [1]. In particular, Majorana zero modes (MZMs), the zero-energy states of the Majorana branch, have attracted much attention since MZMs do not obey ordinary Abelian statistics and can be utilized for quantum computing [2, 3]. Thus, direct detection of MZMs has become a holy grail of current condensed matter physics [4, 5]. Half-quantum fluxoid (HQF) [6] in a spin-triplet superconductor or a superfluid is known to host such MZMs [7, 8].

An additional phase degree of freedom in a superconducting wave function is the key ingredient for the realization of HQF states. For a spin-singlet superconducting ring with wave function $\psi_S = |\Delta_S|e^{i\theta}$, the single-valuedness of ψ_S requires quantization $\Phi' = n\Phi_0$ (integer-quantum fluxoid, IQF) inside a closed path. Here, n is an integer, Φ' is the fluxoid, and $\Phi_0 = h/2e$ is the flux quantum with h the Planck constant and e the elementary charge. Note that, in a superconductor smaller than the penetration depth, the fluxoid, which contains an integration of the supercurrent along a closed path, is quantized, rather than the flux. For a spin-triplet equal-spin pairing (ESP) superconductor, the wavefunction $\psi_T = |\Delta_T|(-e^{i\theta_\uparrow}|\uparrow\uparrow\rangle + e^{i\theta_\downarrow}|\downarrow\downarrow\rangle)$ has two phase degrees of freedom. In an ESP ring, half-integer quantization $\Phi' = n'\Phi_0$ with $n' = \pm 1/2, \pm 3/2, \dots$ is allowed even under the constraint of the single-valuedness of the wave function. Such a fluxoid state is called the HQF state.

One of the materials that can host the HQF is Sr_2RuO_4 , which is a leading candidate spin-triplet ESP superconductor [9, 10]. This oxide has a layered perovskite structure and exhibits superconductivity below 1.5 K. Various experiments have provided firm evidence for the spin-triplet ESP state [11–18], but there still are several issues that cannot be understood within the current spin-triplet scenario [19–23]. Also, signatures of HQF have been observed in microstructured Sr_2RuO_4 rings using cantilever magnetometry [24]. Still, in order to come to Majorana braiding, electrical detection of the HQF state is required.

For this, small samples are necessary in order to reduce the spin-current energy of the HQF state, as pointed out by Chung *et al.* [25]. The role of the Zeeman field to lower the kinetic energy of a HQF state is discussed by Vakaryuk and Leggett [26]. Accordingly, a transition from IQF to HQF is expected to occur with increasing in-plane field, with free-energy minima for the HQF states appearing in the middle of neighboring IQF states [Fig. 6.1(a)]. There is a proposal for detection of HQF using perforated films [27]; here we use a simpler system of a ring shape. It should also be mentioned that a superconducting state can exist with an enhanced transition

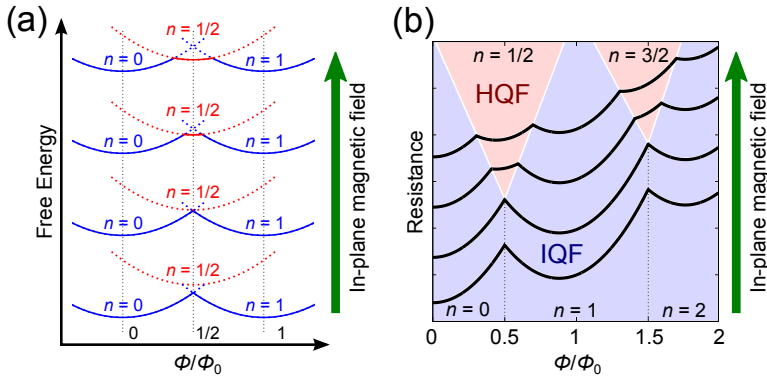


Figure 6.1: (a) Schematic profile of the free energies for IQF states and a HQF state. A HQF state may become energetically favorable under in-plane magnetic field; it is realized above a threshold in-plane field value. (b) Expected change of the magnetoresistance oscillations. Peak splittings with in-plane field are expected when HQF states are realized.

temperature, the so-called 3-K phase. This is observed in eutectic crystals [28–30] or in bulk crystals under uniaxial strain [31–33].

Fluxoid quantization can be investigated by measuring magnetoresistance oscillations as a function of a field applied along the axis of the ring in the regime of the resistive transition, known as the Little-Parks (LP) oscillations [34]. The LP oscillations originate from the oscillations in the free energy and hence in the transition temperature T_c , caused by field-induced supercurrents that flow to satisfy the quantization condition. Then the magnetoresistance curve should trace the field dependence of the free energy [Fig. 6.1]. Thus, a resistance peak in the LP oscillations, located at the border of two neighboring IQF states, should split when HQF states are realized, as shown in Fig. 6.1(b). There are indications that the order parameter in the 3-K phase is not ESP [33, 35]. However, the LP oscillations are robust, regardless of the pairing symmetry or the number of components of the order parameter.

Although techniques to detect the LP oscillations have been developed over the past 50 years, all reported experiments have been performed using superconducting films. To the best of our knowledge, there is no report of the observation of proper LP oscillations even for IQF in a ring made of bulk single crystals, including Sr_2RuO_4 . For Sr_2RuO_4 , although its superconducting thin films have been reported [36, 37], films with strong and homogeneous superconductivity are still virtually absent. Therefore, for LP experiments, techniques to make micro rings without using thin films are needed. Recently, Cai *et al.* reported observation of magnetoresistance oscillations in micro rings made of single-crystalline Sr_2RuO_4 [38, 39]. However, the oscillation amplitudes were substantially larger than the LP expectation.

Here, we report the first observation of proper Little-Parks oscillations in micro rings

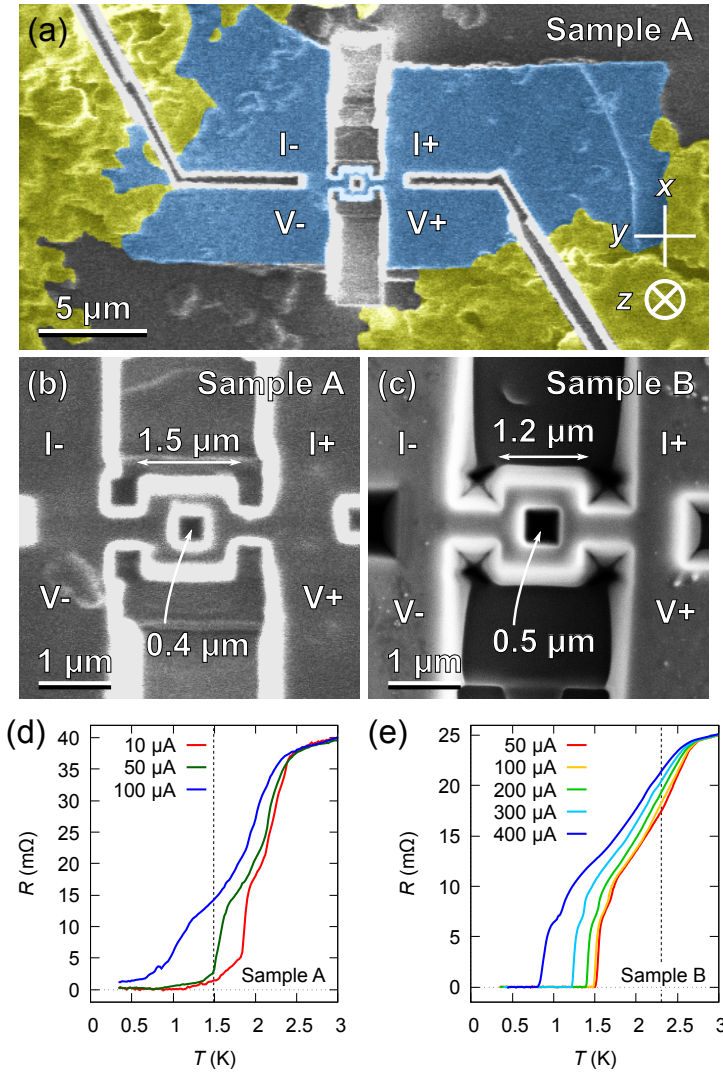


Figure 6.2: (a) False-colored scanning ion microscope (SIM) image of Sample A (yy075). The blue- and yellow-colored regions are the Sr_2RuO_4 crystal and the silver paint, respectively. (b) Magnified SIM image of Sample A. (c) Scanning electron microscope (SEM) image of Sample B (yy150). The thickness of Samples A and B are 1.3 and 2.0 μm , respectively. Resistance of (d) Sample A and (e) Sample B as functions of temperature. Both rings show superconducting transition above 1.5 K and several other transition steps. The dashed lines indicate the temperatures at which the magnetoresistance and magnetovoltage shown in Fig. 6.3 are measured.

of single-crystalline Sr_2RuO_4 . With in-plane fields, we observed two different kinds of peak splittings of the LP oscillations: after careful examination of the raw voltage, we conclude that the splitting in small in-plane fields is extrinsic, originating from asymmetry in the current-voltage characteristics; whereas the splitting in larger in-

plane fields, observable also in the raw voltage, is intrinsic.

6.2. RESULTS AND DISCUSSION

In this study, Sr_2RuO_4 single crystals grown with the floating-zone method [40] were used for micro rings. Before the fabrication, T_c of the crystal C391, used for Sample B, was confirmed to be 1.50 K [Fig. S4] using AC susceptibility method (Quantum Design, PPMS adiabatic demagnetization refrigerator option) [41]. A 1- μm -thin crystal was selected among crushed single crystals, and it was placed on a SrTiO_3 substrate, which has a thermal contraction matching with that of Sr_2RuO_4 . (For Sample A, however, a sapphire substrate with a smaller thermal contraction was used). The surface of the crystal was protected by evaporating a thin layer of SiO_2 after electrodes of high-temperature-cure silver paint (Dupont, 6836) are provided. To fabricate rings with a four-terminal configuration [Figs. 6.2(a)-(c)], the Ga-based focused ion beam (FIB) technique was used with a 20-pA and 30-kV beam. The rings were cooled down to 0.3 K with a ^3He refrigerator (Oxford Instruments, Heliox). To avoid influence of thermoelectric voltage, the resistance was measured under DC current with sign flip: We measure voltage under positive current $V_+ = V(+I)$ and under negative current $V_- = V(-I)$, and evaluate the resistance R as $R = (V_+ - V_-)/2I$. To investigate the field dependence, however, it is crucially important to examine V_+ and V_- individually since LP oscillations are not necessarily invariant under reflection, as seen below. In other words, it is essential to examine magnetovoltage rather than magnetoresistance. Temperature stability during a magnetotransport measurement is approximately 100 μK . This value is substantially smaller than the expected transition-temperature shift due to the LP oscillations, estimated to be around 10 mK. The magnetic field was applied with a three-axes superconducting vector magnet (1 T / 0.2 T / 0.2 T), allowing us to control the out-of-plane and in-plane fields independently. More details on the experimental method are described on the Supplemental Material [42].

Figures 6.2(d) and (e) show the temperature dependence of the ring resistance $R(T)$. Zero resistance due to superconductivity was observed in both rings. Note that the superconducting transitions start well above 1.5 K. This is a signature of the 3-K phase, which is induced in our rings probably by local strain, caused by the FIB process. Several transition steps are observed in both rings. Each step corresponds to the transition of a certain region of the device, as demonstrated in a LP experiment using a conventional superconductor [43]. Still, the correspondence is not entirely straightforward and we rather identify the contribution from the ring by finding the temperature regime where field-induced resistance oscillations occur. In Sample A this is around 1.5 K. In Sample B it is around 2.5 K, while the transitions below 2 K probably are connected to the neck part and the contact part of the structure [Fig. S6].

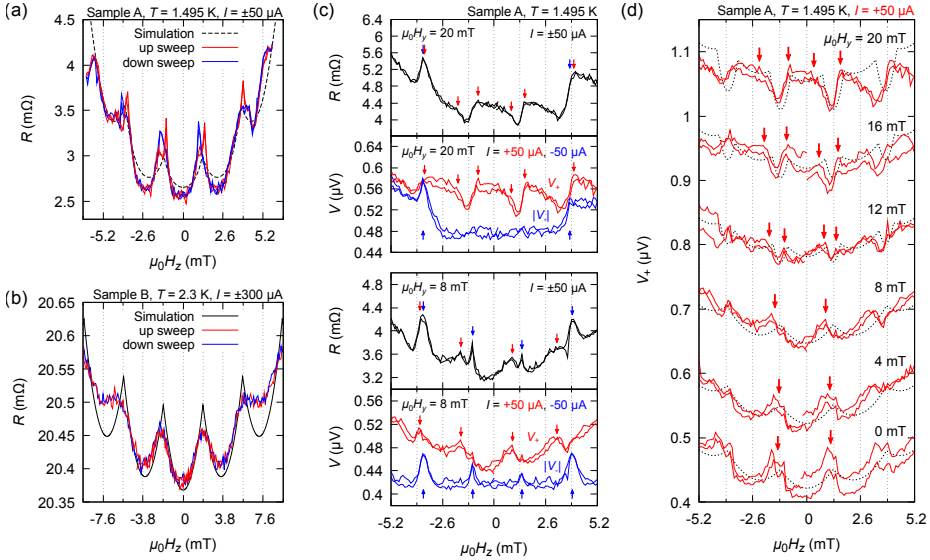


Figure 6.3: Magnetoresistance $R(H_z)$ of (a) Sample A and (b) Sample B without in-plane fields. Both oscillatory periods and amplitudes agree with those of simulations for the Little-Parks oscillations. (c) Comparison of resistance and voltage as functions of H_z for up-sweeps at 0.3 mT/min under constant in-plane fields H_y . At $\mu_0 H_y = 8 \text{ mT}$, the difference in the peak positions in $V_+(H_z)$ and $V_-(H_z)$ results in apparent resistance-peak-splitting because the resistance is evaluated as $(V_+(H_z) - V_-(H_z))/2I$. For $\mu_0 H_y = 20 \text{ mT}$, however, dips at $\mu_0 H_z = \pm 1.3 \text{ mT}$ are clearly observed even in the raw voltage V_+ . Hence the HQF dips in the resistance is not an artifact originating from averaging. Note that for V_- , its absolute values $|V_-|$ are plotted with vertical offsets. (d) Effects of in-plane magnetic field H_y on the magnetovoltage $V_+(H_z)$ of Sample A, including the data shown in (c). Magnetovoltage peaks split above $\mu_0 H_y = 12 \text{ mT}$ as indicated with arrows, and the width of the splitting becomes wider with increasing H_y , as expected for HQF states. Measurements are repeated twice in each conditions to demonstrate good reproducibility. Each set of curves has a $0.1\text{-}\mu\text{V}$ offset for clarity. The dashed curves are guide to the eye.

The magnetoresistance of the rings in the regions of the resistive transitions is shown in Figs. 6.3(a) and (b). The measurements were performed at fixed temperatures indicated with dashed lines in Figs. 6.2(d) and (e). The samples were heated above 5 K before each measurement, then cooled under zero magnetic field. Periodic oscillations were observed with periods $\mu_0 \Delta H = 2.6 \text{ mT}$ and 3.8 mT for Samples A and B, respectively. From ΔH , we can estimate the area S that causes the oscillations by using the relation $\Phi_0 = \mu_0 \Delta H \cdot S$. As a result, we obtain $S_{\text{SampleA}} = 0.80 \mu\text{m}^2$ and $S_{\text{SampleB}} = 0.54 \mu\text{m}^2$, which agree well with the geometry of the rings.

Next, we quantitatively evaluate the oscillations. The shift of T_c due to the fluxoid quantization is given by [44]

$$\frac{T_c(H) - T_c(0)}{T_c(0)} = - \left(\frac{\pi \xi_0 w \mu_0 H}{\sqrt{3} \Phi_0} \right)^2 - \frac{\xi_0^2}{r_1 r_2} \left(n - \frac{\pi \mu_0 H r_1 r_2}{\Phi_0} \right)^2, \quad (6.1)$$

where ξ_0 is the coherence length at 0 K , r_1 is the inner radius, r_2 is the outer radius, and $w = r_2 - r_1$ is the width of a ring. In our calculation, $\xi_0 = 66 \text{ nm}$ (the coherence length along the ab -plane of Sr_2RuO_4 [10]), while we chose $2r_1 = 0.75 \mu\text{m}$, $2r_2 =$

1.4 μm for Sample A, and $2r_1 = 0.7 \mu\text{m}$, $2r_2 = 1.0 \mu\text{m}$ for Sample B. Note that the samples are somewhat "conical", with a smaller top and larger bottom. To convert the T_c shift to a resistance shift, we assume that the shape of a $R(T)$ curve does not change under magnetic field, and the curve shifts to the left by $T_c(0) - T_c(H_z)$. As presented in Figs 6.3(a) and (b) the obtained $R(H_z)$ simulations agree well with the experimental results without any adjustable parameters. We observed oscillations corresponding to $|n| \leq 5$ for Sample A and $|n| \leq 3$ for Sample B. This is because the parabolic component due to the Meissner effect (the first term in Eq. (1)) is dominant at a high field region, and the oscillation component (the second term in Eq. (1)) is not resolved. Though a modulation of the oscillatory period is known in a wide-arm ring [45], we do not observe such non-periodic oscillations. We emphasize again that we succeeded in observing the LP oscillations using a bulk single crystal unlike the other reported LP experiments using superconducting films [46]. Thus, the first conclusion of this paper is that the magnetoresistance oscillations observed in both Sr_2RuO_4 micro rings are the proper LP oscillations.

We then performed magnetotransport measurements with additional in-plane magnetic fields H_y (which is along the current direction). The magnetoresistance as well as the raw voltages V_+ and V_- for $\mu_0 H_y = 8$ and 20 mT are shown in Fig. 6.3(c). The out-of-plane magnetic field values were corrected for the misalignment of the rings with respect to the magnets. To be specific, the actual out-of-plane field H_z is given by $H_z = H_z^{\text{magnet}} \cos\theta + H_y^{\text{magnet}} \sin\theta + H_z^{\text{remnant}}$, where the misalignment angle $\theta = 0.86^\circ$ and the remnant field $H_z^{\text{remnant}} = -0.3$ mT are chosen so that the peaks are located at the same $|H_z|$ value ¹.

For $\mu_0 H_y = 8$ mT, the magnetoresistance $R(H_z)$ peaks appear split at $\mu_0 H_z = \pm 1.3$ mT, which correspond to the transition fields between $n = 0$ and $n = \pm 1$ fluxoid states. However, this peak splitting is not observed in the magnetovoltage $V_+(H_z)$ or $V_-(H_z)$. Instead, the peaks for $V_+(H_z)$ and $V_-(H_z)$ emerge at different H_z . Notice that, the resistance is obtained from an average of V_+ and $-V_-$. As a result, the difference of the peak position in $V_+(H_z)$ and $-V_-(H_z)$ causes artifact peak splitting in the magnetoresistance. Thus, to find an intrinsic peak splitting originating from HQFs, not only $R(H_z)$ but also $V_+(H_z)$ and $V_-(H_z)$ data should be carefully examined: current-averaged resistance data may cause misinterpretation of experimental results.

For $\mu_0 H_y = 20$ mT the situation is different. In this case the splitting in $R(H_z)$ is also observed in $V_+(H_z)$ (see the top two panels of Fig. 6.3(c)). Thus, this splitting is not an artifact originating from the asymmetric peaks in $V_+(H_z)$ and $V_-(H_z)$. In the rest of this paper, we focus on this splitting in the magnetovoltage.

¹In-plane field value is also corrected using $H_y = H_y^{\text{magnet}} \cos\theta - H_z^{\text{magnet}} \sin\theta$. The mixed component $\mu_0 H_z^{\text{magnet}} \sin\theta$ is only 0.078 mT even at the highest H_z^{magnet} value, which is comparable with the geomagnetic field (~ 0.05 mT). Therefore, the in-plane magnetic field can be regarded as constant during the H_z sweep.

Figure 6.3(d) shows the $V_+(H_z)$ with 4-mT H_y steps. Under zero in-plane magnetic field, the oscillations are consistent with the ordinary LP magnetovoltage oscillations with a period corresponding to Φ_0 . When the in-plane field is applied above 12 mT, the peaks in $V_+(H_z)$ clearly start to split. Furthermore, the width of the splitting becomes larger with increasing in-plane field. The increased splitting is consistent with the expectation that the free energy of a HQF state becomes smaller under the in-plane field, as shown in Fig. 6.1. Interestingly, the dips at $\mu_0 H_z = \pm 1.3$ mT for $\mu_0 H_y = 20$ mT are even deeper than the voltage bottoms of the IQF states. Within the HQF scenario, this suggests that the energy of HQF states can become smaller than that of IQF states. We emphasize that the results are well reproducible. The measurements were repeated twice in each condition, and the obtained curves precisely match each other. Magnetoresistance measurements with another in-plane field direction and on Sample B were also performed [42]. For Sample B we do not see signatures of the HQF state in the field range where we expect them, although some sort of splitting occurs above 150 mT.

It may be argued that, if several transition steps in $R(T)$ contribute to the $V_+(H_z)$ and $V_-(H_z)$, the voltages may exhibit a complicated shape resembling that of a HQF state. However, even with 20 mT in-plane field, the resistance is still lower than $6\text{ m}\Omega$ as shown in the upper panel of Fig. 6.3(c). Figure 6.2(d) shows that the resistance corresponding to the lowest-temperature transition is $R < 10\text{ m}\Omega$. Therefore, magnetoresistance measurements were always performed at the sharp transition region occurring around 1.5 K and the higher-temperature transitions do not contribute the magneto-transport.

Let us here compare our results with the previous cantilever magnetometry study by Jang *et al.* [24]. Their measurements were performed at 0.6 K, much lower than T_c . In contrast, our experiment was conducted around T_c to measure finite resistance/voltage. Besides, the measurement current may interact with the circulating supercurrent in our measurements. In spite of these differences, additional features at $\pm\Phi_0/2$ are present in both experiments. Moreover, in both cases the HQF features are only observed with $\mu_0 H_y$ above around 10 mT. Together, the data suggest that the HQF states are very likely to be intrinsic to Sr_2RuO_4 .

There are still issues to be resolved. First, hysteresis is observed in the H_z sweep [Figs. S6-S9]. Such hysteresis between fluxoid states may occur because of the metastable branches in the free energy (dotted parts of the curves in Fig. 6.1(a)). Nevertheless, a detailed mechanism for the asymmetric hysteresis especially at large H_y is still unclear. We comment here that similar hysteresis was also observed in the torque experiment [24]. Second, the splittings of the magnetovoltage peaks for positive H_y are observed only in V_+ but not in V_- . Nevertheless, for negative H_y , peaks in V_- show splitting but not in V_+ [Figs. S6 and S7]. This result ensures the expected symmetry under the concurrent inversion of magnetic field and current: $\mathbf{H} \rightarrow -\mathbf{H}$

and $\mathbf{I} \rightarrow -\mathbf{I}$, $V_{\pm}(\mathbf{H}) \simeq -V_{\mp}(-\mathbf{H})$. On the other hand, the dips in voltages are affected under y -direction field inversion: $H_y \rightarrow -H_y$, $V_{\pm}(H_z, H_y) \neq V_{\pm}(H_z, -H_y)$. Perhaps, one needs to consider the role played by the geometrical asymmetry, for example inhomogeneity in T_c or difference in the effective width between the positive- and negative- x halves of the ring. Finally, the question can be raised why we do not observe the large magnetoresistance oscillations seen by Cai *et al.* [38, 39]. We have also investigated circular rings (rather than the square ones discussed here), and observed no LP oscillations but large amplitude magnetoresistance oscillations. A detailed comparison and its possible origin will be discussed in a subsequent paper.

In conclusion, we have observed the LP oscillations with expected amplitudes and periods in micro rings of Sr_2RuO_4 . This is the first report of the LP oscillations using any bulk single-crystal superconductor. Furthermore, by applying in-plane magnetic fields, we observed splitting of the peaks of the LP magnetovoltage oscillations. The widening of the splitting with increasing in-plane field agrees with the expectation for the HQF state.

REFERENCES

- [1] X.-L. Qi and S.-C. Zhang, *Rev. Mod. Phys.* **83**, 1057 (2011).
- [2] D. A. Ivanov, *Phys. Rev. Lett.* **86**, 268 (2001).
- [3] M. Stone and S. B. Chung, *Phys. Rev. B* **73**, 014505 (2006).
- [4] V. Mourik, K. Zuo, S. M. Frolov, S. R. Plissard, E. P. A. M. Bakkers, and L. P. Kouwenhoven, *Science* **336**, 1003 (2012).
- [5] S. Nadj-Perge, I. K. Drozdov, J. Li, H. Chen, S. Jeon, J. Seo, A. H. MacDonald, B. A. Bernevig, and A. Yazdani, *Science* **346**, 602 (2014).
- [6] G. Volovik and V. Mineev, *JETP Letters* **24**, 561 (1976).
- [7] N. Read and D. Green, *Phys. Rev. B* **61**, 10267 (2000).
- [8] C. Kallin and J. Berlinsky, *Reports on Progress in Physics* **79**, 054502 (2016).
- [9] A. P. Mackenzie and Y. Maeno, *Rev. Mod. Phys.* **75**, 657 (2003).
- [10] Y. Maeno, S. Kittaka, T. Nomura, S. Yonezawa, and K. Ishida, *J. Phys. Soc. Jpn.* **81**, 011009 (2012).
- [11] K. Ishida, H. Mukuda, Y. Kitaoka, K. Asayama, Z. Q. Mao, Y. Mori, and Y. Maeno, *Nature* **396**, 658 (1998).
- [12] G. Luke, Y. Fudamoto, K. Kojima, M. Larkin, J. Merrin, B. Nachumi, Y. Uemura, Y. Maeno, Z. Mao, Y. Mori, H. Nakamura, and M. Sigrist, *Nature* **394**, 558 (1998).
- [13] J. A. Duffy, S. M. Hayden, Y. Maeno, Z. Mao, J. Kulda, and G. J. McIntyre, *Phys. Rev. Lett.* **85**, 5412 (2000).
- [14] J. Xia, Y. Maeno, P. T. Beyersdorf, M. M. Fejer, and A. Kapitulnik, *Phys. Rev. Lett.* **97**, 167002 (2006).
- [15] S. Kashiwaya, H. Kashiwaya, H. Kambara, T. Furuta, H. Yaguchi, Y. Tanaka, and Y. Maeno, *Phys. Rev. Lett.* **107**, 077003 (2011).
- [16] M. S. Anwar, S. R. Lee, R. Ishiguro, Y. Sugimoto, Y. Tano, S. J. Kang, Y. J. Shin, S. Yonezawa, D. Manske, H. Takayanagi, T. W. Noh, and Y. Maeno, *Nat. Commun.* **7**, 13220 (2016).
- [17] M. Manago, K. Ishida, Z. Mao, and Y. Maeno, *Phys. Rev. B* **94**, 180507 (2016).
- [18] M. Manago, T. Yamanaka, K. Ishida, Z. Mao, and Y. Maeno, *Phys. Rev. B* **94**, 144511 (2016).

- [19] C. W. Hicks, J. R. Kirtley, T. M. Lippman, N. C. Koshnick, M. E. Huber, Y. Maeno, W. M. Yuhasz, M. B. Maple, and K. A. Moler, *Phys. Rev. B* **81**, 214501 (2010).
- [20] S. Yonezawa, T. Kajikawa, and Y. Maeno, *Phys. Rev. Lett.* **110**, 077003 (2013).
- [21] S. Yonezawa, T. Kajikawa, and Y. Maeno, *J. Phys. Soc. Jpn.* **83**, 083706 (2014).
- [22] S. Kittaka, A. Kasahara, T. Sakakibara, D. Shibata, S. Yonezawa, Y. Maeno, K. Tenya, and K. Machida, *Phys. Rev. B* **90**, 220502 (2014).
- [23] E. Hassinger, P. Bourgeois-Hope, H. Taniguchi, S. René de Cotret, G. Grissonnanche, M. S. Anwar, Y. Maeno, N. Doiron-Leyraud, and L. Taillefer, *Phys. Rev. X* **7**, 011032 (2017).
- [24] J. Jang, D. G. Ferguson, V. Vakaryuk, R. Budakian, S. B. Chung, P. M. Goldbart, and Y. Maeno, *Science* **331**, 186 (2011).
- [25] S. B. Chung, H. Bluhm, and E.-A. Kim, *Phys. Rev. Lett.* **99**, 197002 (2007).
- [26] V. Vakaryuk and A. J. Leggett, *Phys. Rev. Lett.* **103**, 057003 (2009).
- [27] V. Vakaryuk and V. Vinokur, *Phys. Rev. Lett.* **107**, 037003 (2011).
- [28] Y. Maeno, T. Ando, Y. Mori, E. Ohmichi, S. Ikeda, S. NishiZaki, and S. Nakatsuji, *Phys. Rev. Lett.* **81**, 3765 (1998).
- [29] M. S. Anwar, T. Nakamura, S. Yonezawa, M. Yakabe, R. Ishiguro, H. Takayanagi, and Y. Maeno, *Scientific Reports* **3**, 2480 (2013).
- [30] Y. Ying, N. Staley, Y. Xin, K. Sun, X. Cai, D. Fobes, T. Liu, Z. Mao, and Y. Liu, *Nat. Commun.* **4** (2013).
- [31] S. Kittaka, H. Taniguchi, S. Yonezawa, H. Yaguchi, and Y. Maeno, *Phys. Rev. B* **81**, 180510 (2010).
- [32] C. W. Hicks, D. O. Brodsky, E. A. Yelland, A. S. Gibbs, J. A. N. Bruin, M. E. Barber, S. D. Edkins, K. Nishimura, S. Yonezawa, Y. Maeno, and A. P. Mackenzie, *Science* **344**, 283 (2014).
- [33] A. Steppke, L. Zhao, M. E. Barber, T. Scaffidi, F. Jerzembeck, H. Rosner, A. S. Gibbs, Y. Maeno, S. H. Simon, A. P. Mackenzie, and C. W. Hicks, *Science* **355**, eaaf9398 (2017).
- [34] W. A. Little and R. D. Parks, *Phys. Rev. Lett.* **9**, 9 (1962).
- [35] M. S. Anwar, R. Ishiguro, T. Nakamura, M. Yakabe, S. Yonezawa, H. Takayanagi, and Y. Maeno, *Phys. Rev. B* **95**, 224509 (2017).

- [36] Y. Krockenberger, M. Uchida, K. Takahashi, M. Nakamura, M. Kawasaki, and Y. Tokura, *Appl. Phys. Lett.* **97**, 2502 (2010).
- [37] J. Cao, D. Massarotti, M. E. Vickers, A. Kursumovic, A. D. Bernardo, J. W. A. Robinson, F. Tafuri, J. L. MacManus-Driscoll, and M. G. Blamire, *Supercond. Sci. Technol.* **29**, 095005 (2016).
- [38] X. Cai, Y. A. Ying, N. E. Staley, Y. Xin, D. Fobes, T. J. Liu, Z. Q. Mao, and Y. Liu, *Phys. Rev. B* **87**, 081104 (2013).
- [39] X. Cai, Y. Ying, B. Zakrzewski, D. Fobes, T. Liu, Z. Mao, and Y. Liu, *arXiv:1507.00326*.
- [40] Z. Mao, Y. Maeno, and H. Fukazawa, *Mater. Res. Bull.* **35**, 1813 (2000).
- [41] S. Yonezawa, T. Higuchi, Y. Sugimoto, C. Sow, and Y. Maeno, *Rev. Sci. Instrum.* **86**, 093903 (2015).
- [42] See Supplemental Material [url] for the details of device fabrication process and additional results to support the conclusion of the main paper, which includes Refs. [48–52].
- [43] G. R. Berdiyrov, S. H. Yu, Z. L. Xiao, F. M. Peeters, J. Hua, A. Imre, and W. K. Kwok, *Phys. Rev. B* **80**, 064511 (2009).
- [44] V. V. Moshchalkov, L. Gielen, C. Strunk, R. Jonckheere, X. Qiu, C. V. Haesendonck, and Y. Bruynseraede, *Nature* **373**, 319 (1995).
- [45] M. Morelle, D. S. Golubović, and V. V. Moshchalkov, *Physical Review B* **70**, 144528 (2004).
- [46] V. V. Moshchalkov and J. Fritzsche, *Nanostructured Superconductors* (World Scientific Publishing, 2011), and the references there in.
- [47] In-plane field value is also corrected using $H_y = H_y^{\text{magnet}} \cos\theta - H_z^{\text{magnet}} \sin\theta$. The mixed component $\mu_0 H_z^{\text{magnet}} \sin\theta$ is only 0.078 mT even at the highest H_z^{magnet} value, which is comparable with the geomagnetic field (~ 0.05 mT). Therefore, the in-plane magnetic field can be regarded as constant during the H_z sweep.
- [48] R. Loetzsch, A. Lübcke, I. Uschmann, E. Förster, V. Große, M. Thuerk, T. Koettig, F. Schmidl, and P. Seidel, *Appl. Phys. Lett.* **96**, 1901 (2010).
- [49] O. Chmaissem, J. D. Jorgensen, H. Shaked, S. Ikeda, and Y. Maeno, *Phys. Rev. B* **57**, 5067 (1998).
- [50] M. Lucht, M. Lerche, H.-C. Wille, Y. V. Shvyd'Ko, H. Rüter, E. Gerda, and P. Becker, *J. Appl. Cryst.* **36**, 1075 (2003).

-
- [51] D. Batchelder and R. Simmons, *J. Chem. Phys.* **41**, 2324 (1964).
- [52] A. P. Mackenzie, R. K. W. Haselwimmer, A. W. Tyler, G. G. Lonzarich, Y. Mori, S. Nishizaki, and Y. Maeno, *Phys. Rev. Lett.* **80**, 161 (1998).

